

Published in final edited form as:

*J Am Chem Soc.* 2012 October 17; 134(41): 17262–17273. doi:10.1021/ja307497h.

## Development of Enantioselective Synthetic Routes to (–)-Kinamycin F and (–)-Lomaiviticin Aglycon

Christina M. Woo, Shivajirao L. Gholap, Liang Lu, Miho Kaneko, Zhenwu Li, P. C. Ravikumar, and Seth B. Herzon\*

Department of Chemistry, Yale University, New Haven, CT 06520, United States

### Abstract

The development of enantioselective synthetic routes to (–)-kinamycin F (**9**) and (–)-lomaiviticin aglycon (**6**) is described. The diazotetrahydrobenzo[*b*]fluorene (diazofluorene) functional group of the targets was prepared by fluoride-mediated coupling of a  $\beta$ -trimethylsilylmethyl- $\alpha,\beta$ -unsaturated ketone (**38**) with an oxidized naphthoquinone (**19**), palladium-catalyzed cyclization (**39**→**37**), and diazo transfer (**37**→**53**). The D-ring precursors **60** and **68** were prepared from *m*-cresol and 3-ethylphenol, respectively. Coupling of the  $\beta$ -trimethylsilylmethyl- $\alpha,\beta$ -unsaturated ketone **60** with the juglone derivative **61**, cyclization, and diazo transfer, provided the advanced diazofluorene **63**, which was elaborated to (–)-kinamycin F (**9**) in three steps. The diazofluorene **87** was converted to the  $C_2$ -symmetric lomaiviticin aglycon precursor **91** by enoxysilane formation and oxidative dimerization with manganese tris(hexafluoroacetylacetonate) (**94**, 26%). The stereochemical outcome is attributed to the steric bias engendered by the mesityl acetal of **87** and contact ion pairing of the intermediates. The coupling product **91** was deprotected (*tert*-butylhydrogen peroxide, trifluoroacetic acid–dichloromethane) to form the chain isomer of lomaiviticin aglycon **98**, which cyclizes to (–)-lomaiviticin aglycon (**6**, 39–41% overall). The scope of the fluoride-mediated coupling process is delineated (nine products, average yield = 72%, Table 2); a related enoxysilane quinonylation reaction is also described (10 products, average yield = 77%, Table 1). We establish that dimeric diazofluorenes undergo hydrodediazotization 3-fold faster than related monomeric diazofluorenes (Table 6). The simple diazofluorene **103** is a potent inhibitor of ovarian cancer stem cells ( $IC_{50}$  = 500 nM).

### Introduction

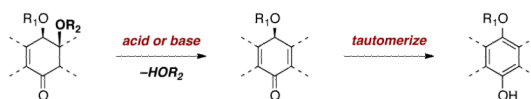
Lomaiviticins A–E (**1–5**, Figure 1) are the most complex members of a family of bacterial metabolites that contain a diazotetrahydrobenzo[*b*]fluorene (diazofluorene) functional group.<sup>1</sup> The lomaiviticins are structurally related to the monomeric diazofluorenes known as the kinamycins (**7–10**).<sup>2</sup> No less than ten distinct kinamycins have been described; kinamycins A (**7**), C (**8**), F (**9**), and the epoxykinamycin FL-120B' (**10**),<sup>3</sup> are representative. The kinamycins and lomaiviticins are potent antiproliferative and antimicrobial agents, and a large body of data now supports bioreductive activation<sup>4</sup> of the diazofluorene as a first step in a cascade leading to cell death.<sup>5</sup> It has been proposed that redox cycling of the quinone to produce reactive oxygen species (ROS),<sup>5a–d</sup> formation of vinyl radical (**11**),<sup>5c,d,e,g,i</sup> *ortho*-quinone methide (**12**),<sup>5c–e,g–i</sup> and acylfulvene (**13**) intermediates by reduction,<sup>4a,5k</sup> or addition of biological nucleophiles to the diazo substituent (**14**),<sup>5b</sup> may contribute to cytotoxicity (Figure 2). The targets of these metabolites are not known; various kinamycins

\*Corresponding Author seth.herzon@yale.edu.

**Supporting Information Available:** Experimental procedures and detailed characterization data of all new compounds. This material is available free of charge via the internet at <http://pubs.acs.org>.

and lomaiviticin A (**1**) are known to cleave dsDNA *in vitro*<sup>1a,5g,i</sup> and in tissue culture<sup>5f</sup> and a protein target has been implicated in the activity of kinamycin F (**9**).<sup>5j</sup>

Synthetic planning toward these targets is significantly complicated by the sensitivity of the diazofluorene toward nucleophiles and reducing agents. In addition, the  $\beta$ -alkoxyenone substructure of lomaiviticin A (**1**) is unstable toward an elimination–aromatization pathway (eq. 1), which limits the range of conditions that are compatible with late-stage intermediates. Moreover, syntheses and installation of the carbohydrate residues of the lomaiviticins, in particular, the  $\beta$ -linked 2,6-dideoxyaminoglycoside residue, is



expected to be challenging. Finally, formation of the central and highly congested bridging carbon–carbon bond in the lomaiviticins constitutes perhaps the most significant obstacle toward their synthesis.

To date, several completed routes to the kinamycins<sup>6</sup> and studies toward the lomaiviticins<sup>7</sup> have been described. Our own efforts have resulted in an efficient synthesis of (–)-kinamycin F (**9**),<sup>8d</sup> the first synthesis of (–)-lomaiviticin aglycon (**6**),<sup>7i</sup> and the development of a general and versatile strategy to prepare diazofluorenes of wide structural variability. We have discovered several new reactions during our investigations, have obtained insights into the factors influencing reductive activation of the diazofluorene, and have identified certain diazofluorenes as potent inhibitors of ovarian cancer stem cells. The full details of these investigations are described below.

## Results and Discussion

### Development of a Convergent and Versatile Route to the Diazofluorene

**Function**—Given the substantial body of evidence implicating the diazofluorene in the biological effects of the kinamycins and lomaiviticins, a versatile strategy to access this functional group was deemed valuable. We targeted diazofluorenes represented by the generalized structure **15** (Scheme 1). Deconstruction of **15** by excision of dinitrogen and a one-carbon synthon, followed by separation of the naphthoquinone and enone residues, formed the hypothetical synthetic precursors **16** and **17**. Initial efforts focusing on appending the one-carbon synthon and dinitrogen substituents to the naphthoquinone **16** were unsuccessful.<sup>8</sup> Therefore, we pursued a strategy comprising addition of the one-carbon substituent to the enone, followed by bond formation to the quinone, as discussed below.

In preliminary studies, we employed the hydrazone **18** (Scheme 2), which was obtained in one step from cyclohex-2-ene-1-one.<sup>9</sup> The hydrazone and enoxysilane functions of **18** were envisioned to serve as handles for bond formation to the naphthoquinone. We discovered that activation of **18** with tris-(diethylamino)sulfonium difluorotrimethylsilicate [TASF(Et)]<sup>10</sup> in the presence of 5,8-dimethoxy-2,3-dibromonaphthoquinone (**19**)<sup>11</sup> cleanly formed the  $\alpha$ -quinonylated product **20** in 73% yield as a single detectable *anti* diastereomer (<sup>1</sup>H NMR analysis).

A broad range of enoxysilanes undergo  $\alpha$ -quinonylation in high yield (Table 1). In cases where the enoxysilane possesses a  $\beta$ -stereocenter, the coupling products were formed with high *anti* selectivity (>5:1; entries 2,3,5,7, and **20**, 72–85%). Unsymmetrical naphthoquinones couple with regiocontrol, provided that the starting reagent contains a

substituent to differentiate the 2- and 3-positions (entries 4, 5, 61%, 76%). Enoxysilanes derived from cyclopentanone (entry 6, 85%), acyclic ketones (entry 9, 82%), and heterocyclic ketones (entry 10, 85%) are also competent nucleophiles.  $\alpha$ -Quaternary ketones are formed in good yield (entry 8, 65%). Common methods for the construction of carbon–carbon bonds to quinones include metal-catalyzed cross-coupling reactions,<sup>12</sup> lithiation of halogenated hydroquinone ethers,<sup>13</sup> and the oxidative addition of boronic acids.<sup>14</sup> This fluoride-mediated coupling reaction provides a useful complement to these protocols.

Synthesis of the quinonylated ketone **20** was encouraging since it contained all of the carbon atoms of our target. We envisioned forming the final ring by intramolecular 1,4-addition of the hydrazone to the naphthoquinone, followed by loss of hydrogen bromide (**20**→**31**, Scheme 3). However, under a variety of conditions, the cyclization product **31** could not be formed (UPLC/MS analysis), potentially due to the *anti* arrangement of the quinone and hydrazone substituents of **20**.<sup>8</sup>

We next targeted the  $\beta$ -methyl- $\alpha$ - $\beta$ -unsaturated ketone **35** (Scheme 4). We envisioned forming an extended enolate of **35**, followed by 5-*endo*-trig cyclization to construct the tetracycle **36**. The precursor **34** was synthesized by copper-catalyzed 1,4-addition of methyl magnesium chloride to cyclohex-2-ene-1-one, trapping with chlorotrimethylsilane, and coupling with **19** (80% overall). Although we were unable to oxidize **34** by several conventional methods, we discovered that thermolysis of **34** under an atmosphere of dioxygen formed the oxidation product **35** (13% yield). Heating solutions of **35** in the presence of palladium (II) acetate, bis(diphenylphosphino)ferrocene, and potassium carbonate afforded the hydroxyfulvene **37** in 77% yield. Attempts to cyclize **35** using bases alone were unsuccessful.

The cyclization product **37**, and structurally-related intermediates (vide infra), exist exclusively in the hydroxyfulvene (e.g., **37**) rather than the keto tautomer (**36**, Scheme 4). Substituent-dependent ketone–hydroxyfulvene equilibria have been reported for related structures.<sup>5h</sup> In the present system, the hydroxyfulvene tautomer may be stabilized by intramolecular hydrogen-bonding and  $\pi$ -conjugation of the hydroxy group with the carbonyl substituents. Although we had made substantial progress toward our target, the low efficiency of the oxidation step (**34**→**35**) led us to reorganize the sequence of bond-forming events. Three considerations were critical in the development of our successful approach. First, we recognized that reoxidation (e.g., palladium acetate<sup>15</sup> or benzeneselenyl chloride–hydrogen peroxide<sup>16</sup>) of conjugate addition products such as **33** provides a route to  $\beta$ -substituted- $\alpha,\beta$ -unsaturated ketones that circumvents the difficult oxidation observed above (**34**→**35**). Second, the fluoride-mediated quinonylation reaction appeared to be unique in its ability to unite the enone and quinone fragments, and we sought to retain this chemistry. Finally, although not mechanistically well-understood, the palladium-catalyzed cyclization (**35**→**37**) provided an efficient method to forge the cyclopentadiene ring of the target.

With these considerations in mind, the  $\beta$ -trimethylsilylmethyl- $\alpha,\beta$ -unsaturated ketone **38** was synthesized by copper-catalyzed 1,4-addition of trimethylsilylmethyl magnesium chloride to **32**, trapping with chlorotrimethylsilane, and reoxidation (76% overall, Scheme 5). TASF(Et)-mediated coupling of **38** with 2,3-dibromo-5,8-dimethoxynaphthoquinone (**19**) proceeded smoothly, to afford the ketoquinone product **39** (85%). The observed preference for  $\gamma$ -quinonylation may be steric in origin.

This  $\gamma$ -quinonylation reaction is also relatively general (Table 2). A variety of  $\beta$ -trimethylsilylmethyl- $\alpha,\beta$ -unsaturated ketones, including those with quaternary carbon centers (entries 1, 2, 7, 8, 57–96%), acetal (entries 3, 4, 83%, 85%, respectively), *para*-methoxybenzyl ether (entries 6, 7, 99%, 65%, respectively), and ester substituents (entry 8,

96%), couple in high yields. As in our  $\alpha$ -quinonylation reaction, unsymmetrical, electronically-biased naphthoquinones react with regiocontrol (entry 4, 85%). 3-(Trimethylsilylmethyl)-cyclopent-2-ene-1-one is also a competent nucleophile for this reaction (entry 5, 67%). Nucleophiles bearing  $\alpha$ -substitution, however, couple in diminished yields (entry 9, 22%), and the presence of a ketone substituent appears to be essential to achieve activation of the allylsilane function (entry 10). We have recently found that the bench-stable, commercially available salt *tetra*-butylammonium difluorotriphenylsilicate (TBAT),<sup>17</sup> may be employed in place of TASF(Et) (entries 1, 3).

With the ketoquinone **39** in hand, we investigated methods to forge the final carbon–carbon bond of the diazofluorene (**39**→**37**). Surprisingly, the conditions employed for the cyclization of **35** were ineffective (entry 1, Table 3). Further optimization was conducted with stoichiometric palladium to facilitate accurate measurement. Among a variety of ligands and palladium precursors examined, the combination of palladium (II) acetate and triphenylphosphine emerged as the most promising. Using these reagents and cesium carbonate as base, the hydroxyfulvene **37** was isolated in 31% yield (entry 2). Triethylamine (TEA, entry 3) and silver phosphate (entry 4) were less effective. By employing silver carbonate as base, raising the temperature to 80 °C, and using polymer-supported triphenylphosphine (PS-PPh<sub>3</sub>, to simplify purification), the isolated yield of **37** was increased to 40% (entry 6). The low isolated yield of **37** was attributed to formation of the palladium complex **52**, identified by UPLC/MS analysis and accounting for a significant mole fraction of **37** at these high loadings of palladium. Complexes between the structurally related anthracyclines and palladium are known.<sup>18</sup> Although we were unable to ascertain the nature of the bonding interactions in **52** (e.g.  $\eta^5$ ,  $\kappa^2$ ), attempts to displace the product **37** by addition of excess acetylacetone or bis(diphenylphosphino)ferrocene were unsuccessful. The substrate **50**, which bears a quaternary center on the D-ring, formed the cyclization product **51** in 79% yield (entry 7), and a complex with palladium could not be detected during the reaction mixture (UPLC/MS analysis). Using this substrate, we were also able to decrease the loading of palladium to 25 mol% (86% yield of **51**, entry 8). In general, cyclization of substrates bearing a quaternary center on the D-ring, including those employed en route to the targets (vide infra), are much more efficient than simple model systems such as **39**.

Diazo transfer to the hydroxyfulvene **37** was all that was required to complete the synthesis of the diazofluorene. Historically, an early application of *para*-toluenesulfonyl azide (*p*-TsN<sub>3</sub>), by Doering,<sup>19</sup> was in the synthesis of diazocyclopentadiene itself from lithium cyclopentadienide. The conjugate base of **37** possesses five inequivalent cyclopentadienide carbon atoms, but only addition to the desired position generates a stable diazo adduct. Exposure of the hydroxyfulvene **37** to triethylamine and common diazotransfer agents, such as methanesulfonylazide (MSA),<sup>20</sup> *p*-acetamidobenzenesulfonyl azide (*p*-ABSA),<sup>21</sup> or *p*-TsN<sub>3</sub>,<sup>19</sup> afforded low yields of the diazofluorene product **53** (entries 1–3, Table 4, 4–20%). Use of the more electrophilic imidazole-1-sulfonylazide hydrochloride (ISA)<sup>22</sup> formed the diazofluorene **53** in 74% yield in less than one hour at 0 °C (entry 4). Trifluoromethanesulfonyl azide (TfN<sub>3</sub>)<sup>23</sup> and nonaflyl azide<sup>24</sup> were slightly more effective (81%, 85%, entries 5, 6 respectively). The latter is preferred due to its increased thermal stability and lower volatility.

The chemistry outlined above has allowed us to prepare a large variety of monomeric diazofluorenes. The antiproliferative activity of many of these compounds has been evaluated, and certain synthetic diazofluorenes have emerged as potent inhibitors of cancer stem cells (vide infra). Of greatest significance, these studies laid the foundation for syntheses of (–)-kinamycin F (**9**) and (–)-lomaiviticin aglycon (**6**), as described in detail below.

**Syntheses of the Enone Fragments**—Our route to the diazofluorene defined the enone fragments required for syntheses of kinamycins and lomaiviticins, and these were prepared by the routes outlined in Scheme 6. Beginning with *m*-cresol (kinamycin series), silyl ether formation (*tri*-isopropylsilyl chloride, imidazole) and Birch reduction (lithium, ammonia) formed the cyclohexadiene **54** (99%, two steps). Regio- and stereoselective asymmetric dihydroxylation<sup>25</sup> then generated the vicinal diol **56** in 66% ee (55% yield). The use of the *tri*-isopropylsilyl protecting group was critical to the success of this step; presumably, its steric bulk prevents entry of the enoxysilane into the binding pocket of cinchona alkaloid–osmium complex, allowing selective oxidation of the less reactive alkene. The modest enantiomeric excess observed in this transformation was attributed to the negligible steric requirements of the methyl substituent, which renders discrimination of the faces of the alkene difficult. No attempt to optimize the enantiomeric excess was made, as we found that subsequent intermediates were highly crystalline and could be resolved to 97% ee.

The diol **56** was then transformed to the acetonide **58** by stirring with 2,2-dimethoxypropane and pyridinium *para*-toluenesulfonate (PPTS, 88%). Treatment of **58** with phenylselenium chloride formed the  $\alpha$ -selenyl ketone **59** (69%, >20:1 mixture of diastereomers). Finally, oxidation of **59** (hydrogen peroxide, pyridine) and thermal elimination of the resulting selenyl oxide formed an enone (not shown) that was homologated by copper-catalyzed 1,4-addition of trimethylsilyl methylmagnesium chloride, trapping with chloro trimethylsilane, and reoxidation (**60**, 73% over two steps).

In the lomaiviticin series, silylation and Birch reduction of 3-ethylphenol provided the diene **55** (>99%). Asymmetric dihydroxylation of **55** formed the diol **57** (62%, 91% ee). Derivatives of **57** were used in our lomaiviticin studies (vide infra).

**Completion of (–)-Kinamycin F (9)**—To complete the synthesis of (–)-kinamycin F (**9**), a suitable naphthoquinone coupling partner, biased toward addition at the C-3 position, was required.<sup>8</sup> Toward this end, *O*-(methoxymethyl)-2-bromo-3-methoxyjuglone (**61**) was prepared by heating a methanolic solution of *O*-(methoxymethyl)-2,3-dibromo-juglone and sodium carbonate (96%).<sup>8</sup> Fluoride-mediated coupling with the  $\beta$ -trimethylsilylmethyl- $\alpha,\beta$ -unsaturated ketone **60** proceeded with complete regioselectivity, forming the C-3 substituted product **62** in 79% yield (Scheme 7). The cyclization and diazotransfer steps proceeded smoothly, as in our model system, to form the diazofluorene **63** (65%, two steps). To complete the synthesis we needed to develop a method for the stereocontrolled conversion of the ketone function of **62** to a *trans*-1,2-diol. Site-selectivity in the reduction step was a serious concern, as an earlier study by Feldman and Eastman<sup>5c,d</sup> had established the diazofluorene as highly reactive toward reducing agents. To control selectivity, we pursued an  $\alpha$ -oxidation, directed reduction sequence. Treatment of the diazofluorene **63** with *tri*-isopropylsilyl trifluoromethanesulfonate (TIPSOTf) and di-isopropylethylamine (DIPEA) formed an enoxysilane (not shown) that was exposed to an excess of dimethyldioxirane in a mixture of methylene chloride and methanol at –40 °C. Under these conditions, the free  $\alpha$ -hydroxy ketone **65** was obtained, presumably formed by in situ methanolysis of the silyloxy epoxide **64**. The stereoselectivity of this oxidation [verified by successful conversion of **65** to (–)-kinamycin F (**9**)] is consistent with faster addition of the dioxirane to the convex face of the *cis*-fused 6-5 system. The  $\alpha$ -hydroxyl group of **65** was then used to control selectivity in the reduction step.

We considered several reagents known to effect the directed reduction of  $\alpha$ - and  $\beta$ -hydroxy ketones. This reaction is most commonly accomplished with tetramethylammonium triacetoxyborohydride,<sup>26</sup> but the use of acetic acid as cosolvent was undesirable. We employed borane•tetrahydrofuran complex, as this reagent had been shown to effect the directed reduction of  $\alpha$ -hydroxy ketones, though the stereoselectivity for simple

cycloalkanones was low.<sup>27</sup> To implement the reduction, the  $\alpha$ -hydroxyketone **65** was dissolved in tetrahydrofuran and cooled to  $-78\text{ }^{\circ}\text{C}$ . Borane•tetrahydrofuran complex (1 equiv) was added, and the resulting mixture was warmed to  $-20\text{ }^{\circ}\text{C}$ . Under these conditions the *trans*-1,2-diol **67** was formed in 58% yield. Minor amounts (<5%) of quinone reduction products were detected by UPLC/MS analysis, suggesting that the reduction proceeds via the in situ generated borinite ester **66**. To complete the synthesis, the diol **67** was deprotected by treatment with hydrochloric acid in methanol at low temperature, to provide (–)-kinamycin F (**9**) in 65% yield.

**Synthesis of (–)-Lomaiviticin Aglycon (6)**—With a route to the kinamycins established, we focused on the preparation of (–)-lomaiviticin aglycon (**6**). When we began our studies we hypothesized that, given the existence of the kinamycins, nature may synthesize lomaiviticins A (**1**) and B (**2**) by oxidative coupling of monomeric diazofluorenes (see Supporting Information for a working mechanism for the putative biosynthetic dimerization). Accordingly, we considered several synthetic methods to effect this transformation. Direct oxidative coupling of cycloalkanones,<sup>28</sup> oxidative coupling of ketone, ester, and amide enolates,<sup>29</sup> and single electron oxidation of enoxysilane<sup>30</sup> or enamine<sup>31</sup> derivatives all had precedent. Two considerations led us to focus on enoxysilane coupling pathways. First, in our kinamycin work, we discovered that  $\beta$ -oxygenated enoxysilanes (Scheme 7) derived from protected diazofluorenes could be generated in near quantitative yield. Second, we expected that  $\beta$ -elimination would be problematic using enolate-based methods.

In a model study, we found that enoxysilanes derived from simple diazofluorenes could be oxidatively coupled in good yield.<sup>8</sup> This motivated us to study this transformation in more detail using a fully-functionalized substrate, and the diazofluorene **71** was prepared by the sequence outlined in Scheme 8. Oxidation<sup>15</sup> of the enoxysilane **57** formed the enone **68** (92%). Treatment of the enone **68** with mesitylaldehyde dimethyl acetal<sup>32</sup> in the presence of PPTS as catalyst formed the acetal **69** (12:1 mixture of *endo* and *exo* isomers, 80%). Homologation, fluoride-mediated coupling with 5,8-bis(methoxymethyl)-2,3-dibromonaphthoquinone (**70**), cyclization, and diazo transfer provided the *endo*-mesityl diazofluorene **71** in 37% overall yield. Treatment of the *endo*-mesityl diazofluorene **71** with *p*-toluenesulfonic acid in methanol formed the (–)-monomeric lomaiviticin aglycon (**72**, 55%).<sup>33</sup> Alternatively, treatment of **71** with TBSOTf and DIPEA formed an enoxysilane (not shown) that was oxidatively coupled (ceric ammonium nitrate) to provide the  $C_2$ -symmetric dimeric product **73** (42%), as well as the monomeric quinone **74** (8%). In these experiments, only a single dimeric product was formed, as determined by <sup>1</sup>H NMR and UPLC/MS analysis of the unpurified reaction mixture. Although the  $C_2$ -symmetry of the product was evident by NMR analysis, this element of symmetry also prevented rigorous assignment of relative stereochemistry. To obtain evidence for stereochemistry, we deprotected the dimer **73** by heating with 20% trifluoroacetic acid in methanol at  $50\text{ }^{\circ}\text{C}$ . Under these strongly acidic conditions, the starting material was converted to the aglycon **75** (41%). This compound was completely characterized by multidimensional NMR analysis, and these data revealed the presence of the C-1/1' carbonyl substituents, providing evidence that ring closure to form the hemiketal structure of lomaiviticin B (**2**) had not occurred. Based on this result, and our kinamycin studies, we assigned the stereochemistry of **75** as the unnatural *anti*, *anti*-configuration. In retrospect, the formation of the *anti*, *anti*-diastereomer **73** is not surprising; the concave topology of the molecule and the steric congestion introduced by the mesityl protecting groups both favor bond formation to the  $\alpha$ -face of the monomer **71**.

Aromatization issues notwithstanding, among several strategies considered to arrive at the natural *syn, syn*-configuration, double-epimerization of the *anti, anti*-aglycon **75** seemed the most straightforward. An extensive battery of conditions were evaluated with the goal of enolizing the ketone functional groups within **75**. We hypothesized that even if the relative energies of the diastereomers were similar, cyclization to form lomaiviticin aglycon (**6**) should drive the equilibrium forward. Unfortunately, however, the *anti, anti*-aglycon **75** exhibited limited stability toward nucleophiles and bases. Under forcing acidic conditions, **75** was remarkably inert. For example, no deuterium incorporation was observed in the  $\alpha$ -positions of **75** after heating with trifluoroacetic acid (20% v/v) in methanol- $d_4$  for 7 min at 120 °C under microwave irradiation ( $^1\text{H}$  NMR analysis).

We then turned our attention toward epimerization of the protected *anti, anti*-dimer **73**. In this case, hemiketal formation is not possible, but we expected that protonation of an enol(ate) from the convex face to afford the desired *syn, syn*-stereochemistry would be kinetically favored. Although this protected intermediate was significantly more robust, activation of the  $\alpha$ -protons was not possible. This may be due to the increased steric bulk about these protons originating from the mesityl acetal protecting groups. After several months of focused experimentation, our epimerization studies were abandoned.

We next explored the installation of a removable functional group at the  $\alpha$ -position of the diazofluorene (Scheme 9). In this approach, the stereochemistry of the resulting dimer would be ultimately controlled by removal of this functional group, rather than the dimerization step. Several  $\alpha$ -functionalized diazofluorenes were prepared from the enoxysilane **76**, including the  $\alpha$ -bromo,  $\alpha$ -fluoro,  $\alpha$ -phenylselenyl, and  $\alpha$ -phenylsulfenyl ketones (**77a–d**, respectively). However, with the exception of the  $\alpha$ -fluoroketone derivative **77b**, all attempts to generate  $\alpha$ -substituted enoxysilanes from these functionalized diazofluorenes were unsuccessful. Although conditions for the reductive cleavage of  $\alpha$ -fluoroketones are not widespread,<sup>34</sup> we attempted to advance the fluorinated product **77b**. Treatment of **77b** with TBSOTf and TEA formed the enoxysilane **78**. Exposure to CAN and sodium bicarbonate formed a single  $C_1$ -symmetric dimeric product **79** (39%). The presence of extensive oxidation and fluorine substituents about the newly-formed bond made complete characterization of **79** difficult, but all NMR data are consistent with carbon–oxygen bond formation (as shown), rather than the expected carbon–carbon coupling product.

Although we were cognizant of the reactivity of the diazofluorene toward reducing agents,<sup>5c,d,g,h</sup> we prepared<sup>8</sup> the  $\alpha$ -phenylselenyl and  $\alpha, \beta$ -epoxy ketones **80** and **81** and examined the possibility of conducting a reductive coupling reaction by formation of an  $\alpha$ -keto radical (Figure 3). Unfortunately, under a variety of reducing conditions<sup>8</sup> extensive decomposition of the substrates was observed. We also attempted the direct oxidative coupling of the monomeric lomaiviticin aglycon (**72**). The flexibility introduced by removal of the cyclic protecting group was anticipated to allow access to the natural *syn, syn*-stereochemistry. However, efforts to dimerize **72**, directly or in the presence of air or added oxidants [CAN, bis(trifluoroacetoxy)iodobenzene, potassium ferricyanide], were unsuccessful. In some instances oxidation to a putative diquinone (UPLC/MS and NMR analysis, not shown) was observed, but this could not be manipulated to a dimeric product.

The extensive studies described above served to define the stability profile of synthetic diazofluorenes: while they were reactive toward reducing agents and nucleophiles, they were robust toward strong oxidants. With this in mind, we prepared the C-3-deoxydiazofluorene **83** (Scheme 10) because we believed that removal of the C-3 oxygen substituent would bias the system for oxidative coupling *anti* to the ethyl substituent, to provide the natural relative configuration. Stereoretentive oxidation of the C-3/3' C–H

bonds of the product would then provide lomaiviticin aglycon (**6**). This strategy found encouraging precedent in the work of Wender and Baran, who had demonstrated that highly selective C–H hydroxylations can be effected in complex settings using dioxirane-based reagents.<sup>35</sup>

The synthesis of the protected C-3/3'-dideoxydimer **84** began with the ketone **82**.<sup>36</sup> Protection of the secondary alcohol (chloromethyl methyl ether, DIPEA) and elaboration as before provided the C-3-deoxydiazofluorene **83** (24% over five steps). Enoxysilane formation (TBSOTf, DIPEA), followed by addition of CAN, formed the oxidative coupling product **84** in 60% yield as a single detectable diastereomer. The relative stereochemistry of **84** was confirmed by observation of a W-plane coupling between the C-2 and C-4 hydrogen atoms. Deprotection of **84** (boron tribromide, dichloromethane) formed C-3/3'-dideoxylomaiviticin aglycon **85** (46%). Unfortunately, neither **84** nor **85** was reactive toward dimethyldioxirane or trifluorodimethyldioxirane, perhaps due to the steric congestion about the targeted C–H bonds.

At this juncture two invariable trends dominated our synthetic planning. First, single electron oxidation of monomeric enoxysilanes was the only method that provided dimeric products. Second, modification of the stereochemistry following the dimerization appeared unachievable. These considerations led us to focus on the synthesis of substrates that might be compatible with the enoxysilane coupling protocol and also provide the natural stereochemistry on dimerization. We considered the use of acyclic protecting groups on the vicinal diol function, however intermediates bearing acyclic alkyl or silyl ether protecting groups were less stable toward elimination of the  $\beta$ -oxygen substituent. The limited stability of the diol **68** prevented installation of smaller (unactivated) cyclic protecting groups, such as formaldehyde acetal.

Inspection of molecular models, and later, computational studies<sup>8</sup> clearly revealed the origins of the steric bias in the dimerization of the *endo*-mesityl diazofluorene **71**. In the energy-minimized structure,<sup>8</sup> the mesityl substituent protrudes into the cavity of the 6-5 system. Approach from the  $\alpha$ -face, to afford the undesired *anti*, *anti*-stereochemistry is kinetically favored. In considering ways to invert this bias, we recognized that epimerization of the mesityl substituent, to the *exo* orientation, might promote bond formation to the desired (concave) face of the enoxysilane. The *exo*-mesityl diazofluorene **87** was prepared by a modification of our route to the *endo*-isomer **71** (Scheme 11). Under conditions developed for protection of the diol **68**, the *endo*-acetal is the kinetically-favored product. Warming of the reaction mixture to 50 °C promotes epimerization of the acetal, to form a 1:1 mixture of *endo* and *exo* diastereomers (**86**). Resubjection of the diastereomerically pure *exo* isomer (obtained by careful purification on ca. 25 mg scales) formed a 1:0.8 mixture of *exo:endo* isomers, suggesting they are nearly equal in energies. In practice, the mixture of *endo* and *exo* acetals **68** (and subsequent intermediates) were advanced through the diazo transfer step, at which point the *endo*- and *exo*-diazofluorenes **71** and **87** were isolated separately.

Ultimately, the diazofluorene **87** was successfully advanced to lomaiviticin aglycon (**6**) by a sequence comprising enoxysilane formation, oxidative dimerization, and deprotection (Scheme 12). Among a large number of oxidants evaluated for their ability to dimerize enoxysilanes derived from **87**, only two, ceric ammonium nitrate (CAN) and manganese hexafluoroacetylacetonate (**94**),<sup>37, 38</sup> were effective [oxidation potentials (vs. Fc) = 0.88 and 0.9 for CAN<sup>39</sup> and **94**,<sup>38</sup> respectively]. Up to six isolable products are obtained in these transformations: the undesired *anti*, *anti* and *syn*, *anti* dimers **90** and **92**, respectively, the desired *syn*, *syn*-dimer **91**, the aromatized–oxidized monomer **74**, and the  $\alpha$ -nitrodiazofluorene **93** (when CAN was employed).



A detailed evaluation of the oxidative dimerization step has revealed that the product distribution, efficiency, and stereoselectivity of the transformation are dependent upon enoxysilane structure (silicon substituents), choice of oxidant, and solvent. Selected experiments that provide an overall representation of the factors influencing this reaction are shown in Table 5. Thus, treatment of the *tert*-butyldimethylsilyl derivative **88** with ceric ammonium nitrate afforded a 24% yield of the undesired *anti*, *anti*-diastereomer **90**, 14% of the  $\alpha$ -nitrodiazofluorene **93**, and extensive amounts of unidentified decomposition products (entry 1). Within the limits of UPLC/MS analysis, no additional dimeric products were formed. Oxidation of **88** with manganese tris(hexafluoroacetylacetonate) (**94**) resulted in aromatization (**74**, 28%) and production of a large amount of unidentified decomposition products; less than 5% of the *anti*, *anti*-diastereomer **90** was formed (entry 2). Oxidation of the trimethylsilyl derivative **89** was much more efficient using **94**, and the undesired *anti*, *anti*-dimer **90** was obtained in 26% yield when dichloromethane was employed as solvent. Encouragingly, oxidation of **89** with CAN formed the three dimeric products **90–92** in 17%, 6%, and 10% yield, respectively, as well as the aromatized monomer **74** (8%) and the diazofluorene **87** (8%, entry 4). By employing the trimethylenoxysilane **89**, manganese tris(hexafluoroacetylacetonate) (**94**) as oxidant, and benzene as solvent, the desired *syn*, *syn* coupling product **91** was obtained as the major product (26%, entry 5). Smaller amounts of the undesired *anti*, *anti*-coupling product **90** (12%) were also isolated, and only trace quantities of the *syn*, *anti*-dimer **92** could be detected under these conditions (UPLC/MS analysis). These latter conditions were reproducibly executed on 100-mg scales.

The complexities of radical cation reactions<sup>40</sup> and low mass balances in entries 1–3 of Table 5 caution against overinterpretation of these results. However, the enhanced *anti*, *anti*-stereoselectivity in the dimerization of **89** using manganese tris(hexafluoroacetylacetonate) (**94**) in benzene (entry 5) compared to dichloromethane (entry 3) may be due to formation of a tight ion pair in which the manganese anion is associated with the convex face of the radical cation.<sup>8</sup> Kochi has shown that ion pairs formed from enoxysilanes are closely associated in non-polar solvents.<sup>41</sup> This association may direct bond formation to the more hindered (concave) face of the substrate. Under identical conditions, oxidation of the trimethylenoxysilane derived from the *endo*-isomer **71** provides the *anti*, *anti*-dimer **73** exclusively (38%),<sup>8</sup> suggesting that the shielding of the *endo*-mesityl substituent overrides the steric encumbrance of the manganese anion.

The final obstacle involved deprotection of the *syn*, *syn*-dimer **91**. While the *anti*, *anti*-dimeric products **73** and **90** were stable toward strongly acidic conditions (vide supra; see Supporting Information for deprotection of **90**), the *syn*, *syn*-dimer **91** decomposed under mildly acidic conditions. We attribute the heightened reactivity of **91** to the *anti* arrangement of the  $\alpha$ -proton and  $\beta$ -oxygen substituents, which facilitates  $\beta$ -elimination. After many experiments that resulted in unidentifiable decomposition products, a useful lead was obtained. Treatment of **91** with excess trifluoroacetic acid in wet dichloromethane at  $-35$  °C resulted in rapid formation of the mono mesityl-protected aglycon **95** (UPLC/MS analysis), which slowly converted to the aromatized aglycon **97** (Scheme 13A). We reasoned that the aromatized product **97** was forming by elimination of the  $\beta$ -oxocarbenium ion **96**. To prevent this, we conducted the deprotection in the presence of a large excess of *tert*-butyl hydroperoxide (Scheme 13B).<sup>42</sup> LC/MS analysis revealed that **95** accumulated under these conditions as well, but now neutralization of the reaction mixture at low temperature ( $-78$  °C) followed by extractive workup provided mixtures of the chain isomer of lomaiviticin aglycon **98** as well as the expected ring isomer **6** (**98:6** = 8–2:1), rather than the dehydrated product **97**. Presumably, under these conditions, the oxocarbenium ion **96** is trapped by the peroxide nucleophile before it has a chance to eliminate.

The chain isomer **98** was characterized by multidimensional NMR analysis, which established the presence of the C-1 carbonyl substituent. Attempted separation of this mixture by preparative thin-layer chromatography resulted in cyclization to form the ring isomer **6** exclusively (39–41% overall).

The aglycon **6** was fully characterized by NMR, IR, and HRMS analysis and all data are consistent with the structure shown. However, we observed some differences in NMR chemical shifts between the bis(hemiketal) core of **6** and those of lomaiviticin B (**2**). In particular, the H-2 and C-2 resonances of **6** are observed at 3.41 and 62.1 ppm, respectively (30% DMF-*d*<sub>7</sub>-CD<sub>3</sub>OD), while those of lomaiviticin B (**2**) are reported to resonate at 2.64 and 44.0 ppm, respectively (CD<sub>3</sub>OD; the aglycon **6** is sparingly soluble in CD<sub>3</sub>OD, which prohibited acquisition of spectroscopic data in this solvent).<sup>1a</sup> The C-2 and H-2 resonances of lomaiviticin aglycon **6** are in good agreement with a model system prepared by Nicolaou and co-workers ( $\delta$  H-2 = 2.87,  $\delta$  C-2 = 60.4, C<sub>6</sub>D<sub>6</sub>)<sup>7a</sup> and NMR spectroscopic data for the chain isomer **98** matched closely those of lomaiviticin A (**1**). To provide further evidence for connectivity and stereochemistry in **4**, we isolated the monomesityl aglycon **95** (Scheme 13A) by arresting the deprotection of **91** prematurely. The <sup>1</sup>H and <sup>13</sup>C resonances within the bis(cyclohexenone) substructure of **95** were resolved in CDCl<sub>3</sub>, and were assigned by multidimensional NMR analysis, providing confirmation of connectivity. An NOE between H-3' and H-1' was observed, providing further confirmation of the *syn, syn*-stereochemistry of the dimerization product **91** (Scheme 13C).

The data above left little doubt as to the structure of synthetic lomaiviticin aglycon **6**. We recognized, however, that natural lomaiviticin B (**2**) was obtained as its bis(trifluoroacetate) salt, following a final HPLC purification step.<sup>1a</sup> To probe for potential effects of charge on chemical shifts, lomaiviticin B (**2**) was obtained by partial hydrolysis of lomaiviticin A<sup>1b</sup> (**1**, trifluoroacetic acid, aqueous methanol, 45 °C, 82%).<sup>8</sup> The H-2 and C-2 resonances (as well as all other resonances) of the bis(trifluoroacetate) salt of lomaiviticin B (**2**) obtained in this way were in exact agreement with literature values. The free base of **2** was obtained by a basic wash. The chemical shifts of H-2 and C-2 of the free base form were in better agreement with (–)-lomaiviticin aglycon (**6**, free base of **2**:  $\delta$  H-2 = 3.64,  $\delta$  C-2 = 71.3, CD<sub>3</sub>OD). Thus, the chemical shift discrepancies observed between (–)-lomaiviticin aglycon (**6**) and natural lomaiviticin B (**2**) are attributed to the charged state of **2** when it was obtained from the producing organism.<sup>1a</sup>

**Hydrodediazotization Studies**—A growing body of data suggests the cytotoxic effects of the kinamycins and lomaiviticins are mediated by a reducing co-factor,<sup>5</sup> and the dimeric and monomeric diazofluorene derivatives prepared above provide an opportunity to probe substituents effects on the redox activity of the diazofluorene. We evaluated the rate of reduction of the unnatural *anti, anti*-aglycon **75**, (–)-lomaiviticin aglycon (**6**), the monomeric lomaiviticin aglycon **72**, and (–)-kinamycin C (**8**) by dithiothreitol (1 equiv) in methanol at 37 °C (Table 6). The *anti, anti*-dimer **75** was studied because it contains the flexibility and conjugated ketone substituents found within lomaiviticin A (**1**). Under these conditions, the *anti, anti*-dimer **75** and the monomeric lomaiviticin aglycon (**72**) undergo hydrodediazotization to form the hydroxyfulvenes **99** and **100**, respectively, and more slowly, the products of methanolysis (**101** and **102**).<sup>5k</sup> Interestingly, these data reveal that the rate of reduction of the *anti, anti*-dimer **75** is ca. 3-fold faster than that of the monomeric lomaiviticin aglycon (**72**). Perhaps more strikingly, under otherwise identical conditions, neither (–)-lomaiviticin aglycon (**6**) nor (–)-kinamycin C (**8**) formed detectable levels of reduction products (UPLC/MS analysis). Collectively, these data suggest that the ketone function of lomaiviticin A (**1**) raises the oxidation potential of the diazofluorene, allowing for facile electron transfer. Additionally, a stabilizing donor–acceptor interaction between

the hydroxyfulvene and the remaining diazofluorene may further promote reductive activation of dimers such as **75**, and lomaiviticin A (**1**). Thus, though lomaiviticins A (**1**) and B (**2**) share a good deal of homology, the additional flexibility present in the structure of lomaiviticin A (**1**) is suggested to enhance the rate of reduction of the metabolite.

**Identification of Simple Diazofluorenes as Potent Inhibitors of Ovarian Cancer Stem Cells**—In parallel with our synthetic studies we have conducted structure–function studies of synthetic diazofluorenes. One aspect of this research has focused on evaluating the activity of our synthetic analogs against cancer stem cells (CSCs), a small population of cells within tumors that are highly tumorigenic and chemoresistant. CSCs have been identified in many different cancers, including ovarian cancer.<sup>43</sup>

We have found that the diazofluorene **103** (Figure 4) potently inhibits the growth of cultured ovarian cancer stem cells (IC<sub>50</sub> = 500 nM). This compound is readily-prepared (500 mg of **103** was synthesized in less than one week in our laboratory).<sup>8</sup> Although the development of **103** as a clinical agent is of interest, of equal or greater significance are identification of the biological mechanisms underlying the cytotoxic effects of **103** in this cell line, an avenue of research we are currently pursuing.

## Conclusion

We have described the evolution of enantioselective synthetic routes to (–)-kinamycin F (**9**) and (–)-lomaiviticin aglycon (**6**). Our synthetic routes were enabled by the development of scalable, efficient, and enantioselective syntheses of the kinamycin and lomaiviticin D-ring precursors **60** and **68**, and implementation of a convergent, three-step strategy for construction of the diazofluorene functional group. Use of substrate control to effect the transformation of the ketone **65** to the *trans*-1,2-diol **67**, in the presence of the redox-sensitive diazofluorene, allowed for a short synthesis of (–)-kinamycin F (**9**, 13 steps from *m*-cresol).

Extensive investigations into the oxidative coupling of monomeric diazofluorenes such as **87** has allowed for a short (11-step) synthesis of (–)-lomaiviticin aglycon (**6**). These studies have revealed a complex relationship between substrate structure and reaction conditions, and stereochemical outcome and product distributions. Ultimately, conditions were found to form a precursor to lomaiviticin aglycon (**6**) in good yield (26–33%), and this was successfully advanced to the target.

Several new reactions, including a novel  $\gamma$ -quinonylation of  $\beta$ -trimethylsilyl-  $\alpha$ -  $\beta$ -unsaturated ketones, and a new  $\alpha$ -quinonylation of enoxysilanes, were developed. In addition, we have described the application of nonafllyl azide as a storable, bench-stable surrogate for the volatile and highly reactive reagent trifluoromethanesulfonyl azide. We have also described the first use of manganese tris(hexafluoroacetylacetonate) (**94**) in the oxidative coupling of enoxysilanes. This reagent possesses physical properties (high solubility in nonpolar solvents and a coordinatively-saturated metal center) that are complementary to more common oxidants (such as CAN), and this reagent may find applications in settings beyond those described here. We have obtained evidence that the flexible, dimeric structure of lomaiviticin A (**1**) may enhance the rate of reductive activation of the metabolite, and we have identified simple diazofluorenes (**103**) as potent inhibitors of ovarian cancer stem cells.

The results reported herein lay the foundation for synthesis of lomaiviticin A (**1**) itself. We have delineated efficient routes to advanced monomeric diazofluorenes and established their stability and reactivity profiles. The successful oxidative coupling of these systems provides

encouragement that the dimerization of fully functionalized (glycosylated) monomeric diazofluorenes may be possible.

## Supplementary Material

Refer to Web version on PubMed Central for supplementary material.

## Acknowledgments

Partial financial support from the American Cancer Society, the National Institute of General Medical Sciences (R01GM090000), the National Science Foundation (Graduate Research Fellowship to C. M. W.), the Searle Scholar Program, and Yale University is gratefully acknowledged. We thank Dr. Gil Mor and Dr. Ayesha Alvero for determining the activity of **103** against ovarian CSCs and Dr. Eric Paulson of the Yale Chemical and Biophysical Instrumentation Center for valuable assistance with NMR. We acknowledge the Developmental Therapeutics Program of the National Cancer Institute for in vivo toxicity analysis of **103**. S.B.H. is a fellow of the David and Lucile Packard and the Alfred P. Sloan Foundations, and is a Camille Dreyfus Teacher-Scholar.

## References

- 1(a). He H, Ding WD, Bernan VS, Richardson AD, Ireland CM, Greenstein M, Ellestad GA, Carter GT. *J. Am. Chem. Soc.* 2001; 123:5362. [PubMed: 11457405] Woo CM, Beizer NE, Janso JE, Herzon SB. *J. Am. Chem. Soc.* Article ASAP, DOI: 10.1021/ja3074984. . For reviews, see: Marco-Contelles J, Molina MT. *Curr. Org. Chem.* 2003; 7:1433. Arya DP. *Top. Heterocycl. Chem.* 2006; 2:129. Nawrat CC, Moody CJ. *Nat. Prod. Rep.* 2011; 28:1426. [PubMed: 21589994] Herzon SB, Woo CM. *Nat. Prod. Rep.* 2012; 29:87. [PubMed: 22037715]
- 2(a). Ito S, Matsuya T, mura S, Otani M, Nakagawa A. *J. Antibiot.* 1970; 23:315. [PubMed: 5458310] (b) Hata T, mura S, Iwai Y, Nakagawa A, Otani M. *J. Antibiot.* 1971; 24:353. [PubMed: 5091211] (c) mura S, Nakagawa A, Yamada H, Hata T, Furusaki A, Watanabe T. *Chem. Pharm. Bull.* 1971; 19:2428. (d) Furusaki A, Matsui M, Watanabe T, mura S, Nakagawa A, Hata T. *Isr. J. Chem.* 1972; 10:173. (e) Cone MC, Seaton PJ, Halley KA, Gould SJ. *J. Antibiot.* 1989; 42:179. [PubMed: 2925509] (f) Seaton PJ, Gould SJ. *J. Antibiot.* 1989; 42:189. [PubMed: 2925510]
- 3(a). Lin H-C, Chang S-C, Wang N-L, Chang L-R. *J. Antibiot.* 1994; 47:675. [PubMed: 8040072] (b) Lin H-C, Chang S-C, Wang N-L, Chang L-R. *J. Antibiot.* 1994; 47:681. [PubMed: 8040073]
- 4(a). Moore HW. *Science.* 1977; 197:527. [PubMed: 877572] (b) Rockwell S, Sartorelli AC, Tomasz M, Kennedy KA. *Canc. Metastasis Rev.* 1993; 12:165.
- 5(a). Arya DP, Jebaratnam DJ. *J. Org. Chem.* 1995; 60:3268. (b) Laufer RS, Dmitrienko GI. *J. Am. Chem. Soc.* 2002; 124:1854. [PubMed: 11866589] (c) Feldman KS, Eastman KJ. *J. Am. Chem. Soc.* 2005; 127:15344. [PubMed: 16262378] (d) Feldman KS, Eastman KJ. *J. Am. Chem. Soc.* 2006; 128:12562. [PubMed: 16984207] (e) Zeng W, Ballard TE, Tkachenko AG, Burns VA, Feldheim DL, Melander C. *Bioorg. Med. Chem. Lett.* 2006; 16:5148. [PubMed: 16870443] (f) O'Hara KA, Wu X, Patel D, Liang H, Yalowich JC, Chen N, Goodfellow V, Adedayo O, Dmitrienko GI, Hasinoff BB. *Free Radic. Biol. Med.* 2007; 43:1132. [PubMed: 17854709] (g) Ballard TE, Melander C. *Tetrahedron Lett.* 2008; 49:3157. (h) Khdour O, Skibo EB. *Org. Biomol. Chem.* 2009; 7:2140. [PubMed: 19421453] (i) Heinecke CL, Melander C. *Tetrahedron Lett.* 2010; 51:1455. (j) O'Hara KA, Dmitrienko GI, Hasinoff BB. *Chem. Biol. Interact.* 2010; 184:396. [PubMed: 20079721] (k) Mulcahy SP, Woo CM, Ding WD, Ellestad GA, Herzon SB. *Chem. Sci.* 2012; 3:1070.
- 6(a). Lei X, Porco JA. *J. Am. Chem. Soc.* 2006; 128:14790. [PubMed: 17105273] Kumamoto T, Kitani Y, Tsuchiya H, Yamaguchi K, Seki H, Ishikawa T. *Tetrahedron.* 2007; 63:5189. Nicolaou KC, Li H, Nold AL, Pappo D, Lenzen A. *J. Am. Chem. Soc.* 2007; 129:10356. [PubMed: 17676854] Woo CM, Lu L, Gholap SL, Smith DR, Herzon SB. *J. Am. Chem. Soc.* 2010; 132:2540. [PubMed: 20141138] Scully SS, Porco JA. *Angew. Chem., Int. Ed.* 2011; 50:9722. For studies toward the kinamycins, see: Chen N, Carriere MB, Laufer RS, Taylor NJ, Dmitrienko GI. *Org. Lett.* 2008; 10:381. [PubMed: 18183994] Scully SS, Porco JA. *Org. Lett.* 2012; 14:2646.

- 7(a). Nicolaou KC, Denton RM, Lenzen A, Edmonds DJ, Li A, Milburn RR, Harrison ST. *Angew. Chem., Int. Ed.* 2006; 45:2076.(b) Krygowski ES, Murphy-Benenato K, Shair MD. *Angew. Chem., Int. Ed.* 2008; 47:1680.(c) Morris WJ, Shair MD. *Org. Lett.* 2008; 11:9. [PubMed: 19061365] (d) Zhang W, Baranczak A, Sulikowski GA. *Org. Lett.* 2008; 10:1939. [PubMed: 18410121] (e) Nicolaou KC, Nold AL, Li H. *Angew. Chem., Int. Ed.* 2009; 48:5860. [PubMed: 19719089] (f) Lee HG, Ahn JY, Lee AS, Shair MD. *Chem. –Eur. J.* 2010; 16:13058. [PubMed: 20976820] (g) Morris WJ, Shair MD. *Tetrahedron Lett.* 2010; 51:4310. [PubMed: 20802782] (h) Herzon SB, Lu L, Woo CM, Gholap SL. *J. Am. Chem. Soc.* 2011; 133:7260. [PubMed: 21280607] (i) Baranczak A, Sulikowski GA. *Org. Lett.* 2012; 14:1027. [PubMed: 22309201]
8. See Supporting Information.
9. Díez E, Fernández R, Gasch C, Lassaletta JM, Llera JM, Martín-Zamora E, Vázquez J. *J. Org. Chem.* 1997; 62:5144.
- 10(a). Middleton, WJ. Tris(substituted amino)sulfonium Salts. U.S. Patent. 3,940,402. 1976. (b) Noyori R, Nishida I, Sakata J. *Tetrahedron Lett.* 1980; 21:2085.(c) Noyori R, Nishida I, Sakata J, Nishizawa M. *J. Am. Chem. Soc.* 1980; 102:1223.
11. Huot R, Brassard P. *Can. J. Chem.* 1974; 52:838.
- 12(a). Tamayo N, Echavarren AM, Paredes MC. *J. Org. Chem.* 1991; 56:6488.(b) Liebeskind LS, Riesinger SW. *J. Org. Chem.* 1993; 58:408.
13. Tietze LF, Gericke KM, Schuberth I. *Eur. J. Org. Chem.* 2007; 2007:4563.
14. Fujiwara Y, Domingo V, Seiple IB, Gianatassio R, Del Bel M, Baran PS. *J. Am. Chem. Soc.* 2011; 133:3292. [PubMed: 21341741]
- 15(a). Ito Y, Hirao T, Saegusa T. *J. Org. Chem.* 1978; 43:1011.(b) Larock RC, Hightower TR, Kraus GA, Hahn P, Zheng D. *Tetrahedron Lett.* 1995; 36:2423.
- 16(a). Reich HJ, Reich IL, Renga JM. *J. Am. Chem. Soc.* 1973; 95:5813.(b) Sharpless KB, Launer RF, Teranishi AY. *J. Am. Chem. Soc.* 1973; 95:6137.
17. Pilcher AS, DeShong P. *J. Org. Chem.* 1996; 61:6901. [PubMed: 11667585]
- 18(a). Fiallo MML, Garnier-Suillerot A. *Biochemistry.* 1986; 25:924. [PubMed: 3964654] (b) Fiallo MML, Garnier-Suillerot A. *Inorg. Chim. Acta.* 1987; 137:119.
19. Doering, W. v. E.; DePuy, CH. *J. Am. Chem. Soc.* 1953; 75:5955.
20. Taber DF, Ruckle RE, Hennessy MJ. *J. Org. Chem.* 1986; 51:4077.
21. Baum JS, Shook BC, Davies HML, Smith HD. *Synth. Commun.* 1987; 17:1709.
22. Goddard-Borger ED, Stick RV. *Org. Lett.* 2007; 9:3797. [PubMed: 17713918]
23. Cavender CJ, Shiner VJ. *J. Org. Chem.* 1972; 37:3567.
24. Zhu S-Z. *J. Chem. Soc., Perkin Trans. 1.* 1994:2077.
25. Kolb HC, VanNieuwenhze MS, Sharpless KB. *Chem. Rev.* 1994; 94:2483.
26. Evans DA, Chapman KT, Carreira EM. *J. Am. Chem. Soc.* 1988; 110:3560.
27. Brown HC, Vogel FGM. *Liebigs Ann. Chem.* 1978:695.
28. Hawkins EGE, Large R. *J. Chem. Soc., Perkin Trans. 1.* 1974:280.
- 29(a). Ito Y, Konoike T, Harada T, Saegusa T. *J. Am. Chem. Soc.* 1977; 99:1487.(b) Baran PS, DeMartino MP. *Angew. Chem., Int. Ed.* 2006; 45:7083.(c) DeMartino MP, Chen K, Baran PS. *J. Am. Chem. Soc.* 2008; 130:11546. [PubMed: 18680297]
- 30(a). Baciocchi E, Casu A, Ruzziconi R. *Tetrahedron Lett.* 1989; 30:3707.(b) Avetta CT, Konkol LC, Taylor CN, Dugan KC, Stern CL, Thomson R. *J. Org. Lett.* 2008; 10:5621.
31. Narasaka K, Okauchi T, Tanaka K, Murakami M. *Chem. Lett.* 1992; 21:2099.
32. Ji N, O'Dowd H, Rosen BM, Myers AG. *J. Am. Chem. Soc.* 2006; 128:14825. [PubMed: 17105291]
33. This compound was previously prepared by Nicolaou and co-workers (ref. 7a), and was previously named “the monomeric unit of lomaiviticin aglycon”. Spectroscopic data for synthetic 72 were in agreement with the material synthesized by Nicolaou and co-workers.
- 34(a). Surya Prakash GK, Hu J, Olah GA. *J. Fluorine Chem.* 2001; 112:355.(b) Hata H, Kobayashi T, Amii H, Uneyama K, Welch JT. *Tetrahedron Lett.* 2002; 43:6099.

- 35(a). Wender PA, Hilinski MK, Mayweg AVW. *Org. Lett.* 2004; 7:79. [PubMed: 15624982] (b) Chen K, Baran PS. *Nature.* 2009; 459:824. [PubMed: 19440196]
36. Ohnemüller UK, Nising CF, Encinas A, Bräse S. *Synthesis.* 2007; 2007:2175.
37. Evans S, Hamnett A, Orchard AF, Lloyd DR. *Faraday Discuss. Chem. Soc.* 1972; 54:227.
38. Bryant JR, Taves JE, Mayer JM. *Inorg. Chem.* 2002; 41:2769. [PubMed: 12005502]
39. Connelly NG, Geiger WE. *Chem. Rev.* 1996; 96:877. [PubMed: 11848774]
40. Schmittel M, Burghart A. *Angew. Chem., Int. Ed.* 1997; 36:2550.
41. Bockman TM, Kochi JK. *J. Chem. Soc., Perkin Trans. 2.* 1996:1633.
42. Myers AG, Fundy MAM, Lindstrom PA Jr. *Tetrahedron Lett.* 1988; 29:5609.
- 43(a). Zhou JB, Zhang Y. *Expet. Opin. Drug. Discov.* 2009; 4:741.(b) Alvero AB, Chen R, Fu H-H, Montagna M, Schwartz PE, Rutherford T, Silasi D-A, Steffensen KD, Waldstrom M, Visintin I, Mor G. *Cell Cycle.* 2009; 8:158. [PubMed: 19158483] (c) Bapat SA. *Reproduction.* 2010; 140:33. [PubMed: 20368192] (d) Wei X, Dombkowski D, Meirelles K, Pieretti-Vanmarcke R, Szotek PP, Chang HL, Preffer FI, Mueller PR, Teixeira J, MacLaughlin DT, Donahoe PK. *Proc. Natl. Acad. Sci. U.S.A.* 2010; 107:18874. [PubMed: 20952655]

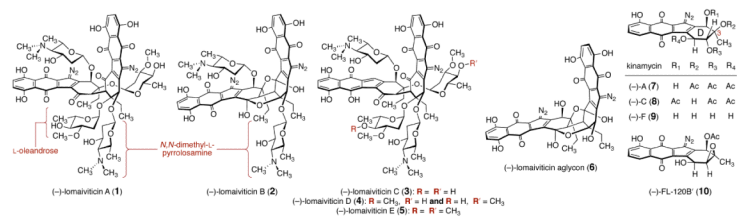


**Figure 1.** Structures of (-)-Lomaiviticins A–E (1–5, respectively), (-)-Lomaiviticin Aglycon (6), (-)-Kinamycins A, C, and F (7–9, respectively), and the Epoxykinamycin (-)-FL-120B' (10).

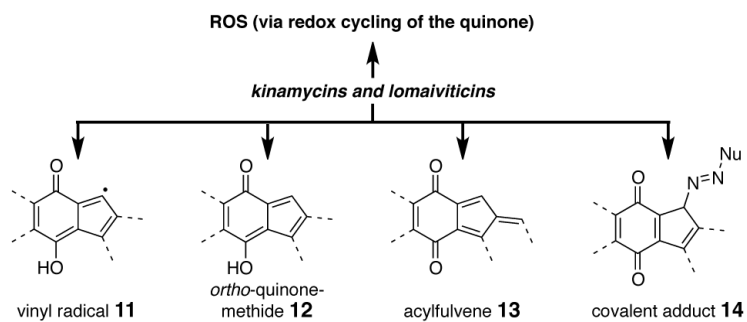


**Figure 2.** Reactive Intermediates Proposed to Form From the Kinamycins and Lomaiviticins.



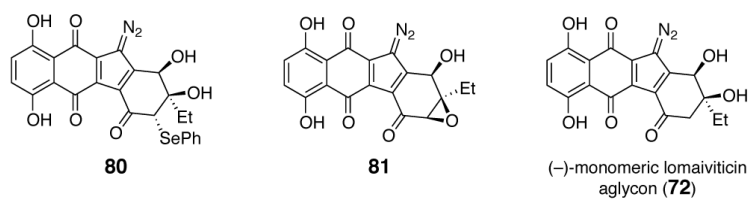


**Figure 3.** Structures of the  $\alpha$ -Phenylselenyldiazofluorene **80**, the  $\alpha, \beta$ -Epoxydiazofluorene **81**, and the Monomeric Lomaiviticin Aglycon (**72**).

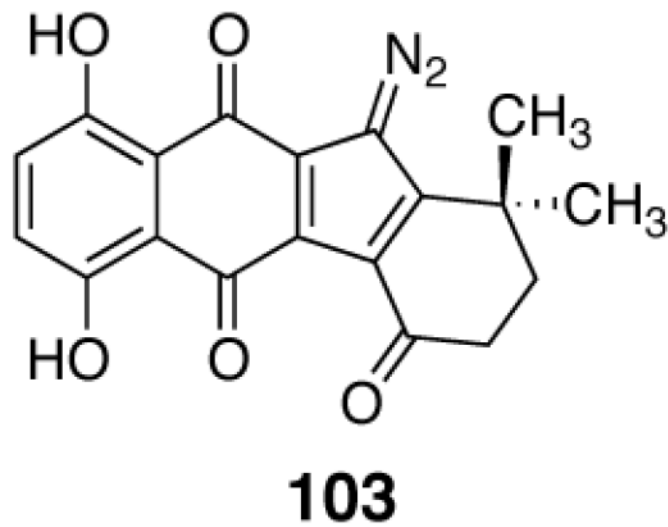
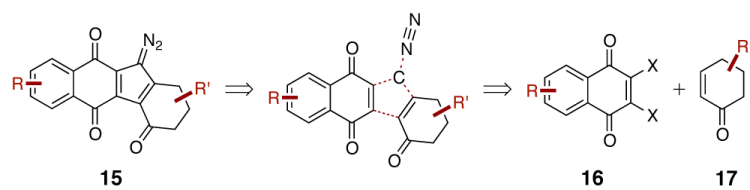


**Figure 4.**  
Structure of the Anti-Cancer Stem Cell Agent **103**.

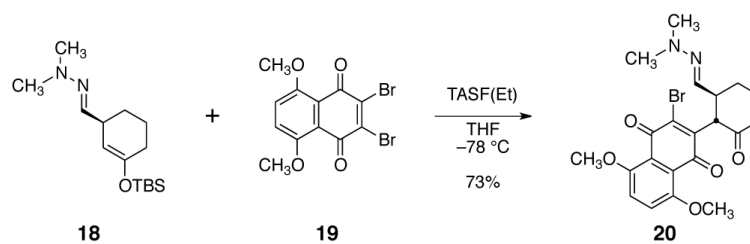


**Scheme 1.**  
Strategy to Access the Diazofluorene Functional Group.

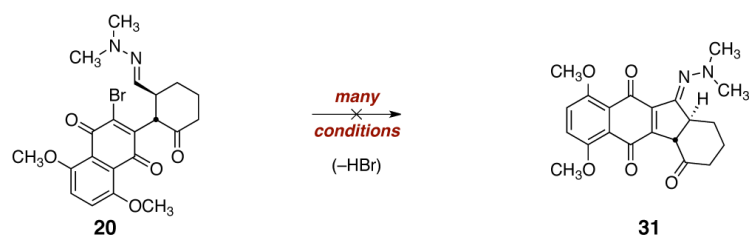
\$watermark-text

\$watermark-text

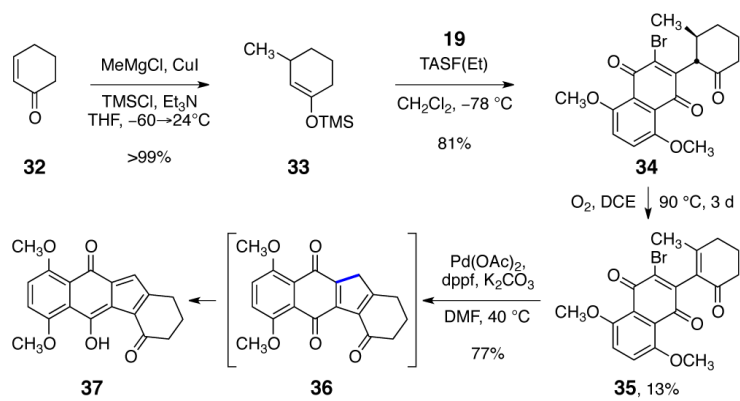
\$watermark-text



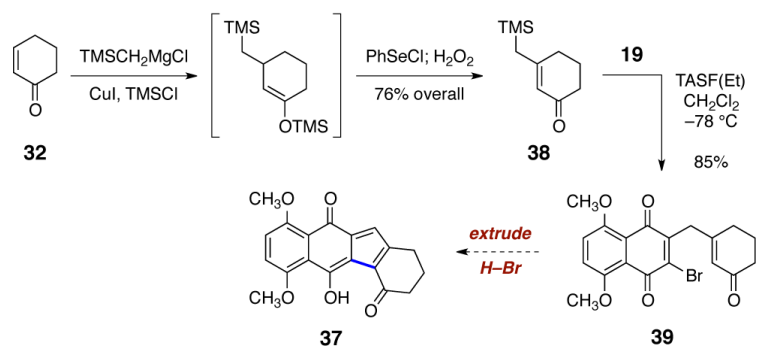
**Scheme 2.**  
Fluoride-Mediated Coupling of the Enoxysilane **18** with 2,3-Dibromo-5,8-dimethoxynaphthoquinone (**19**).



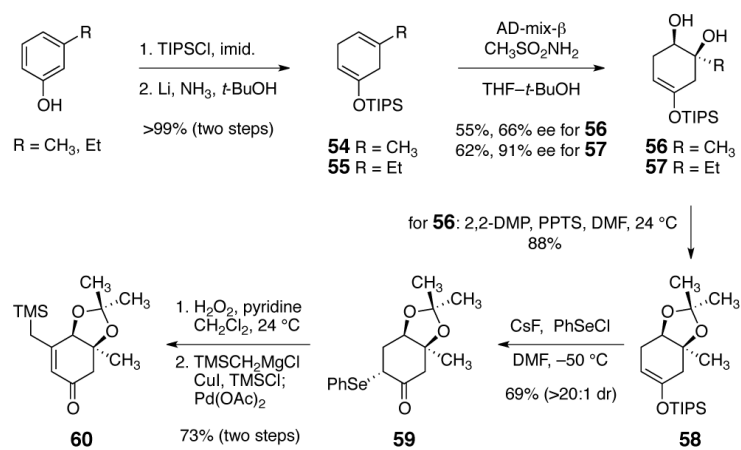
**Scheme 3.**  
Attempted Elaboration of the Hydrazone **20**.



**Scheme 4.**  
Synthesis of the Tetracycline **37**.



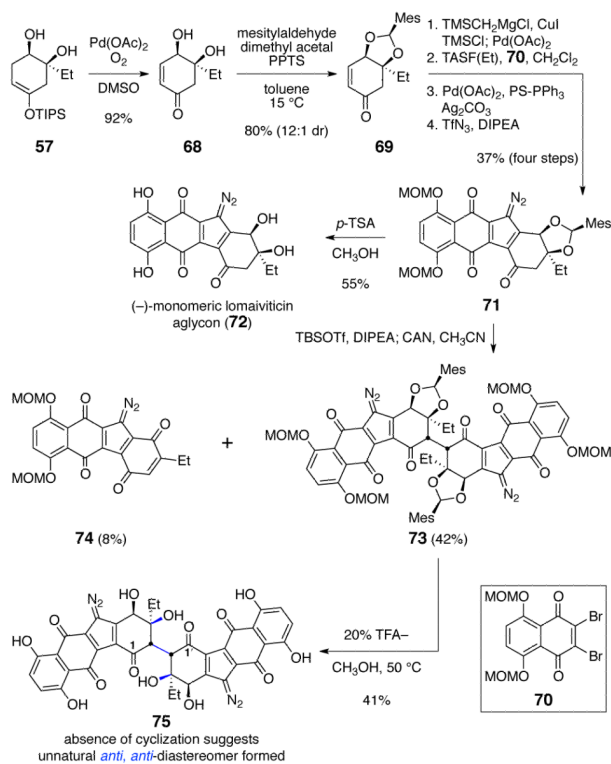
**Scheme 5.**  
Synthesis of the Ketoquinone **39**.



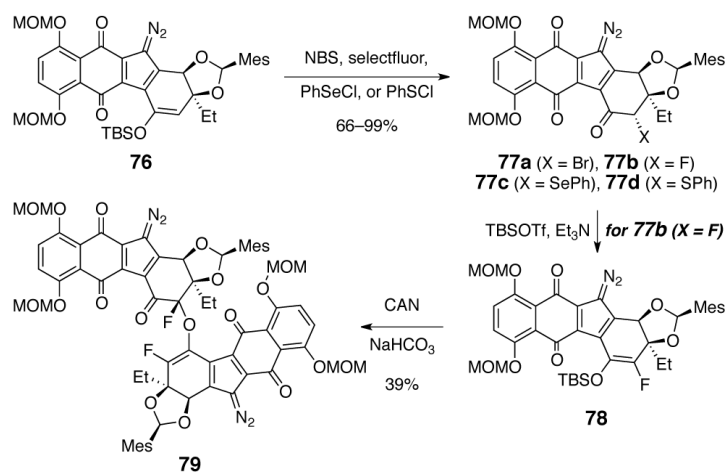
**Scheme 6.**  
Syntheses of the Enone **60**.



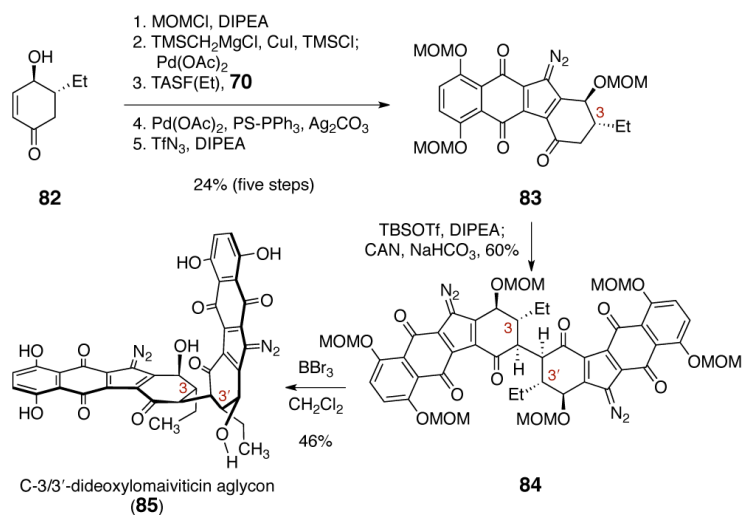




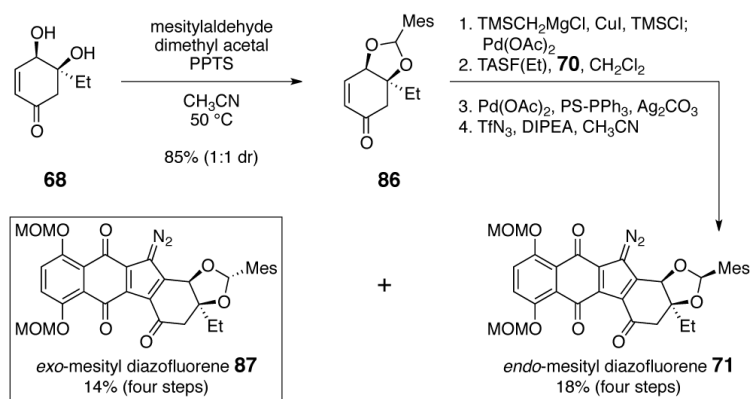
**Scheme 8.** Synthesis and Dimerization of the Bis(methoxymethyl)-*endo*-mesityldiazofluorene **71**.



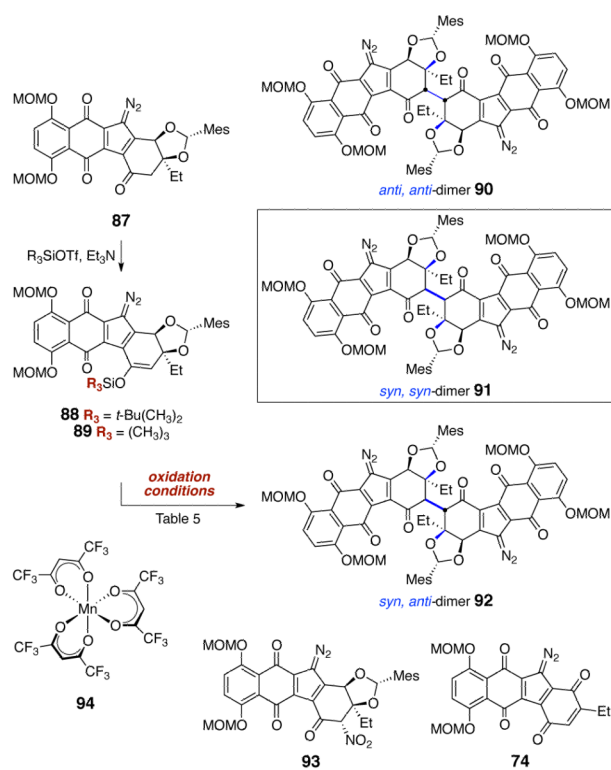
**Scheme 9.**  
Synthesis and Reactions of  $\alpha$ -Functionalized Diazofluorenes **77**.



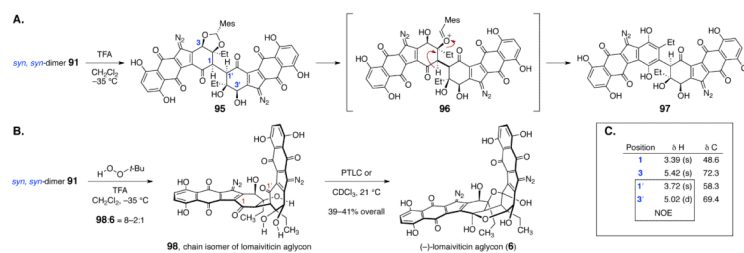
**Scheme 10.**  
 Synthesis of C-3/3'-Dideoxylomaiviticin Aglycon **85**.



**Scheme 11.**  
 Synthesis of the *exo*-Mesityl Diazofluorene **87**.

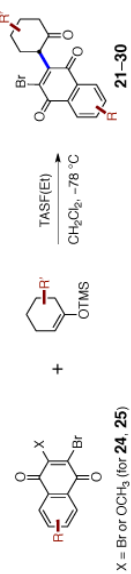


**Scheme 12.**  
 Products Identified in the Oxidative Coupling of the *exo*-Mesityldiazofluorene **87**.

**Scheme 13.**

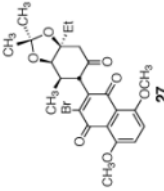
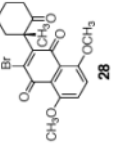
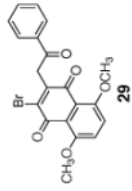
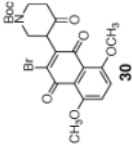
**A.** Deprotection of the *syn, syn*-Dimer **91** (in the Absence of TBHP). **B.** Deprotection of the *syn, syn*-Dimer **91** (in the Presence of TBHP). **C.** Selected  $^1\text{H}$  and NOE NMR Data for the Mono Mesityl-protected Aglycon **95**.

Table 1

Scope of the  $\alpha$ -Quinonylation Reaction.<sup>a</sup>

entry	product	yield	entry	product	yield
1		84%	2 <sup>b</sup>		81%
3 <sup>b</sup>		86%	4		61%
5		76%	6		85%

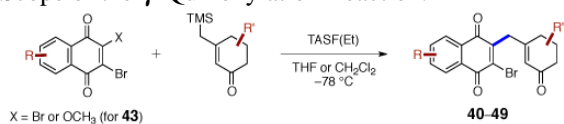


entry	product	yield	entry	product	yield
7		64%	8		65%
9		82%	10		85%

<sup>a</sup> Conditions: TASF(Et) (1.10 equiv), CH<sub>2</sub>Cl<sub>2</sub>, -78 °C.

<sup>b</sup> THF used as solvent.

Table 2

Scope of the  $\gamma$ -Quinonylation Reaction.<sup>a</sup>

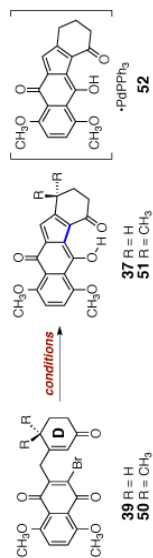
entry	product and yield	entry	product and yield
1	<p><b>40</b> 74%, 65%<sup>b</sup></p>	2	<p><b>41</b></p>
3	<p><b>42</b> 83%, 86%<sup>b</sup></p>	4	<p><b>43</b> 85%</p>
5	<p><b>44</b> 67%</p>	6	<p><b>45</b> 99%</p>
7	<p><b>46</b> 65%</p>	8	<p><b>47</b> 96%</p>
9	<p><b>48</b> 22%</p>	10	<p><b>49</b> nd<sup>c</sup></p>

<sup>a</sup> conditions: TASF(Et) (1.1 equiv), CH<sub>2</sub>Cl<sub>2</sub>, -78 °C.

<sup>b</sup> TBAT (1.1–1.5 equiv), CH<sub>2</sub>Cl<sub>2</sub>, 0 °C.

<sup>c</sup> none detected by <sup>1</sup>H NMR analysis of the unpurified reaction mixture.

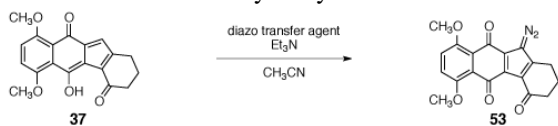
Table 3

Optimization of the Palladium-Mediated Cyclization Reaction.<sup>a</sup>

entry	subs.	solvent	mol% Pd	ligand	base	T (°C)	yield
1	39	DMF	40	dppf	K <sub>2</sub> CO <sub>3</sub>	50	<5%
2	39	THF	80	PPh <sub>3</sub>	C <sub>5</sub> H <sub>5</sub> CO <sub>3</sub>	50	31%
3	39	THF	100	PPh <sub>3</sub>	TEA	50	<5%
4	39	THF	100	PPh <sub>3</sub>	Ag <sub>3</sub> PO <sub>4</sub>	50	dec.
5	39	PhCH <sub>3</sub>	75	PS-PPh <sub>3</sub>	Ag <sub>2</sub> CO <sub>3</sub>	80	22%
6	39	PhCH <sub>3</sub>	100	PS-PPh <sub>3</sub>	Ag <sub>2</sub> CO <sub>3</sub>	80	40%
7	50	PhCH <sub>3</sub>	100	PS-PPh <sub>3</sub>	Ag <sub>2</sub> CO <sub>3</sub>	80	79%
8	50	PhCH <sub>3</sub>	25	PS-PPh <sub>3</sub>	Ag <sub>2</sub> CO <sub>3</sub>	80	86%

<sup>a</sup>Conditions: 1–2 equiv of ligand (with respect to palladium) and 2–3 equivalents of base (with respect to substrate) were employed.

Table 4

Diazo Transfer to the Hydroxyfulvene 37.<sup>a</sup>

entry	diazo transfer agent (equiv)	t (h)	T (°C)	yield
1	MSA (7.5)	4	24	4%
2	<i>p</i> -ABSA (5.0)	1.5	24	20%
3	<i>p</i> -TsN <sub>3</sub> (7.5)	4	24	18%
4	ISA (2.5)	0.3	0	74%
5	TfN <sub>3</sub> (2.5)	0.3	24	81%
6	CF <sub>3</sub> (CF <sub>2</sub> ) <sub>3</sub> SO <sub>2</sub> N <sub>3</sub> (2.5)	0.3	0	85%

<sup>a</sup>Conditions: diazo transfer reagent (2.5–7.5 equiv), TEA (5.0–15 equiv), CH<sub>3</sub>CN.

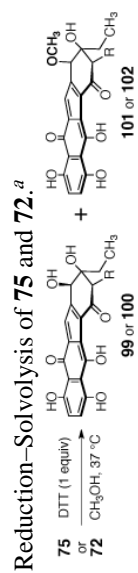
Table 5

Dimerization of the *exo*-Mesityldiazofluorene **87**.<sup>a</sup>

entry	R <sub>3</sub> <sup>b</sup>	oxidant	solvent	90	91	92	74	87
1 <sup>c,d</sup>	<b>88</b>	CAN	CH <sub>3</sub> CN	24%	nd <sup>e</sup>	nd	nd	3%
2 <sup>f</sup>	<b>88</b>	94	PhH	<5%	nd	nd	28%	5%
3 <sup>g</sup>	<b>89</b>	<b>94</b>	CH <sub>2</sub> Cl <sub>2</sub>	26%	nd	<5%	15%	<5%
4 <sup>b</sup>	<b>89</b>	CAN	CH <sub>3</sub> CN	17%	6%	10%	8%	8%
5 <sup>f</sup>	<b>89</b>	<b>94</b>	PhH	12%	26%	<5%	15%	36%

<sup>a</sup> Isolated yields.<sup>b</sup> **88**: R<sub>3</sub> = *t*-Bu(CH<sub>3</sub>)<sub>2</sub>; **89**: R<sub>3</sub> = (CH<sub>3</sub>)<sub>3</sub>.<sup>c</sup> CAN (2.0 equiv), sodium bicarbonate (20 equiv), CH<sub>3</sub>CN, -35 °C.<sup>d</sup> The  $\alpha$ -nitrodiazofluorene **93** was obtained in 14% yield.<sup>e</sup> none detected.<sup>f</sup> Mn(hfacac)<sub>3</sub> (**94**, 1.20 equiv), PhH, 24 °C.<sup>g</sup> Mn(hfacac)<sub>3</sub> (**94**, 1.20 equiv), CH<sub>2</sub>Cl<sub>2</sub>, 24 °C.

Table 6



time (h)	75	99	101	72	100	102
0	100%	0%	0%	100%	0%	0%
1	62%	38%	0%	89%	10%	1%
10	22%	78%	0%	76%	11%	13%

<sup>a</sup> % composition was determined by UPLC/MS analysis.